Table 2. Summary of Proteins with Differential Expression between ASPS Tumor Tissues and Nontumor Tissues

spot no.[a]	accession no.[b]	identified protein	Wilcoxon test p value	fold difference (ratio of means)	pI (cal)[c]	MW (cal) (Da)[c]	protein score[d]	peptide matches	sequence coverage (%)
3552	P07477	trypsin-1	1.5877×10^{-5}	0.008515009	6.08	27111	72	1	8.1
3541	Q9P032	uncharacterized protein C3orf60	1.5877×10^{-5}	0.010363941	8.48	20566	67	1	6
3549	P35030	trypsin-3	1.5877×10^{-5}	0.010390875	7.46	33306	58	1	4.3
3543	Q9NYY3	serine/threonine-protein kinase PLK2	1.5877×10^{-5}	0.011751306	8.52	79270	37	1	1.3
3089	Q99536	synaptic vesicle membrane protein VAT-1	1.5877×10^{-5}	0.021958413	5.88	42122	185	2	8.9
3091	O14773	tripeptidyl-peptidase 1	1.5877×10^{-5}	0.02956955	6.01	61723	149	3	8.2
3539	Q9P1Z9	uncharacterized protein KIAA1529	1.5877×10^{-5}	0.029933118	5.74	192404	40	1	1.2
2792	P07237	protein disulfide-isomerase	1.5877×10^{-5}	0.03101972	4.76	57480	1138	38	35.8
3551	P07477	trypsin-1	1.5877×10^{-5}	0.031037268	6.08	27111	43	1	8.1
3335	P07339	cathepsin D	1.5877×10^{-5}	0.032525296	6.1	45037	254	4	14.3
3090	Q99536	synaptic vesicle membrane protein VAT-1	1.5877×10^{-5}	0.034147549	5.88	42122	225	5	21.4
3556	P16402	histone H1.3	1.5877×10^{-5}	0.035355776	11	22336	32	1	4.1
3544	P47974	butyrate response factor 2	1.5877×10^{-5}	0.036972559	8.52	52000	38	1	5.1
3154	P40121	macrophage-capping protein	3.1754×10^{-5}	0.037782583	5.88	38779	429	8	26.1
2123	Q9H0J4	glutamine-rich protein 2	1.5877×10^{-5}	0.039776539	6.25	181228	42	1	0.5
3560	P07477	trypsin-1	1.5877×10^{-5}	0.041918698	6.08	27111	63	1	8.1
3554	P07477	trypsin-1	1.5877×10^{-5}	0.043031618	6.08	27111	58	1	8.1
3084	Q99536	synaptic vesicle membrane protein VAT-1	1.5877×10^{-5}	0.043691971	5.88	42122	356	7	19.8
3088	Q99536	synaptic vesicle membrane protein VAT-1	1.5877×10^{-5}	0.044704717	5.88	42122	215	5	12.5
3158	P40121	macrophage-capping protein	0.00011114	0.04492316	5.88	38779	332	9	21.8
3504	P23528	cofilin-1	1.5877×10^{-5}	0.046486714	8.22	18719	53	1	6.6
3548	P07477	trypsin-1	1.5877×10^{-5}	0.051111972	6.08	27111	79	1	8.1
1604	P07339	cathepsin D	1.5877×10^{-5}	0.052422591	6.1	45037	91	2	6.3
2015	P01024	complement C3	1.5877×10^{-5}	0.053827382	6.02	188569	58	1	1.3
1488	Q96DA2	Ras-related protein Rab-39B	1.5877×10^{-5}	0.054075741	7.7	24835	36	1	6.1
2791	P07237	protein disulfide-isomerase	1.5877×10^{-5}	0.056152907	4.76	57480	71	2	4.7
2681	P27797	calreticulin	1.5877×10^{-5}	0.059656716	4.29	48283	504	14	26.6
489	P27797	calreticulin	1.5877×10^{-5}	0.059974668	4.29	48283	94	2	4.3
3333	P07339	cathepsin D	1.5877×10^{-5}	0.060978434	6.1	45037	153	4	11.2
3558	P35030	trypsin-3	1.5877×10^{-5}	0.062680878	7.46	33306	60	1	4.3
2976	Q12765	secernin-1	1.5877×10^{-5}	0.062850066	4.66	46980	86	2	6.3
2883	Q6ZMW3	echinoderm microtubule-associated protein-like 6	1.5877×10^{-5}	0.062965523	7.17	220270	50	2	0.4
761	P08670	vimentin	0.0004763	0.065528927	5.06	53676	358	15	23.6
3384	Q9Y5Z4	heme-binding protein 2	1.5877×10^{-5}	0.067161156	4.58	22861	143	2	13.2
1406	Q9NZD8	maspardin	1.5877×10^{-5}	0.068166	5.85	35223	82	1	3.9
3499	Q9P1Z9	uncharacterized protein KIAA1529	1.5877×10^{-5}	0.068985159	5.74	192404	43	1	1.2
1568	Q96C19	EF-hand domain-containing protein D2	1.5877×10^{-5}	0.071337515	5.15	26794	165	3	15
1611	P27348	14-3-3 protein theta	1.5877×10^{-5}	0.074204821	4.68	28032	74	1	5.7
2974	P04264	keratin, type II cytoskeletal 1	1.5877×10^{-5}	0.074765405	8.15	66170	122	2	3.7
3500	P11940	putative protein PABPC1-like	1.5877×10^{-5}	0.075151195	8.88	30256	49	1	7.4
3302	O14646	chromodomain-helicase-DNA-binding protein 1	1.5877×10^{-5}	0.075335702	6.72	197538	40	1	0.5
3562	P07477	trypsin-1	1.5877×10^{-5}	0.076824606	6.08	27111	63	1	8.1
3275	Q9P1Z9	uncharacterized protein KIAA1529	1.5877×10^{-5}	0.07718673	5.74	192404	42	3	1.2
1752	Q7Z6Z7	E3 ubiquitin-protein ligase HUWE1	1.5877×10^{-5}	0.079027202	5.1	485523	39	1	0.3
2846	Q13885	tubulin beta-2A chain	1.5877×10^{-5}	0.079394824	4.78	50274	975	18	43.8
1686	P40121	macrophage-capping protein	1.5877×10^{-5}	0.079825987	5.88	38779	154	4	8.3
3334	P07339	cathepsin D	1.5877×10^{-5}	0.079953736	6.1	45037	310	6	16.5
323	Q8IWE2	protein NOXP20	1.5877×10^{-5}	0.080187134	4.61	61046	267	6	15.1
2558	P14314	glucosidase 2 subunit beta	1.5877×10^{-5}	0.080715302	4.33	60357	316	5	10.6
2794	P07237	protein disulfide-isomerase	1.5877×10^{-5}	0.081241738	4.76	57480	841	25	32.5
326	Q8IWE2	protein NOXP20	1.5877×10^{-5}	0.081614914	4.61	61046	82	2	3.7
2695	P27797	calreticulin	1.5877×10^{-5}	0.083690191	4.29	48283	209	4	9.4
3575	P07477	trypsin-1	0.00019052	0.083697415	6.08	27111	61	1	8.1
3182	Q9UJ70	*N*-acetyl-D-glucosamine kinase	1.5877×10^{-5}	0.084723353	5.81	37694	388	6	25

dx.doi.org/10.1021/pr400929h | *J. Proteome Res.* XXXX, XXX, XXX–XXX

Table 2. continued

spot no.[a]	accession no.[b]	identified protein	Wilcoxon test p value	fold difference (ratio of means)	pI (cal)[c]	MW (cal) (Da)[c]	protein score[d]	peptide matches	sequence coverage (%)
2790	P07237	protein disulfide-isomerase	1.5877×10^{-5}	0.085599608	4.76	57480	313	7	15.4
1877	P62820	Ras-related protein Rab-1A	1.5877×10^{-5}	0.086095703	5.93	22891	216	4	27.3
2971	Q12765	secernin-1	1.5877×10^{-5}	0.087093501	4.66	46980	42	1	2.7
1689	P52565	Rho GDP-dissociation inhibitor 1	1.5877×10^{-5}	0.089182867	5.02	23250	207	5	22.1
2972	Q8N7U6	EF-hand domain-containing family member B	1.5877×10^{-5}	0.089364253	7.5	94558	48	1	1.8
3085	Q99536	synaptic vesicle membrane protein VAT-1	1.5877×10^{-5}	0.090047239	5.88	42122	186	4	17
2841	Q96FT9	uncharacterized protein C14orf179	1.5877×10^{-5}	0.090304869	4.57	23572	44	1	9.1
2124	P60660	myosin light polypeptide 6	1.5877×10^{-5}	0.090851666	4.56	17090	205	4	28.5
2564	P27824	calnexin	1.5877×10^{-5}	0.09097873	4.47	67982	224	4	10.1
2030	Q9H0J4	glutamine-rich protein 2	1.5877×10^{-5}	0.091020777	6.25	181228	45	1	0.5
2839	Q13885	tubulin beta-2A chain	1.5877×10^{-5}	0.091496662	4.78	50274	279	5	11.9
1426	P84157	matrix-remodeling-associated protein 7	1.5877×10^{-5}	0.091543619	4.24	21509	48	1	3.9
992	P60709	actin, cytoplasmic 1	1.5877×10^{-5}	0.092202715	5.29	42052	359	21	21.1
1635	P67936	tropomyosin alpha-4 chain	1.5877×10^{-5}	0.093892535	4.67	28619	613	67	35.1
3441	Q92630	dual specificity tyrosine-phosphorylation-regulated kinase 2	1.5877×10^{-5}	0.094160695	9.7	67123	40	1	4
1128	P40121	macrophage-capping protein	6.3507×10^{-5}	0.094214275	5.88	38779	264	7	14.7
3328	P07339	cathepsin D	1.5877×10^{-5}	0.094241211	6.1	45037	190	4	11.2
3468	Q8WWM9	cytoglobin	1.5877×10^{-5}	0.094317704	6.32	21505	174	4	19.5
1681	P04264	keratin, type II cytoskeletal 1	0.00030166	0.094354027	8.15	66170	807	14	25.6
252	P14625	endoplasmin	1.5877×10^{-5}	0.095256618	4.76	92696	1270	75	33
863	Q07960	Rho GTPase-activating protein 1	1.5877×10^{-5}	0.095902059	5.85	50461	189	6	15.7
3481	P62820	Ras-related protein Rab-1A	1.5877×10^{-5}	0.097286337	5.93	22891	68	1	7.8
3561	P07477	trypsin-1	1.5877×10^{-5}	0.097721585	6.08	27111	67	1	8.1
1292	Q9P1Z9	uncharacterized protein KIAA1529	1.5877×10^{-5}	0.098548367	5.74	192404	43	4	1.2
3573	P07477	trypsin-1	6.3507×10^{-5}	0.098828882	6.08	27111	79	1	8.1
2009	P00441	superoxide dismutase [Cu–Zn]	1.5877×10^{-5}	0.09993381	5.7	16154	44	1	9.1
1836	P51149	Ras-related protein Rab-7a	6.3507×10^{-5}	0.101448964	6.4	23760	421	7	38.2
3263	P47756	F-actin-capping protein subunit beta	1.5877×10^{-5}	0.101659636	5.36	31616	102	2	8.7
1843	P51149	Ras-related protein Rab-7a	3.1754×10^{-5}	0.101686834	6.4	23760	262	6	37.7
2837	Q13885	tubulin beta-2A	1.5877×10^{-5}	0.101856539	4.78	50274	459	11	24
758	P14625	endoplasmin	6.3507×10^{-5}	0.101899313	4.76	92696	245	6	7.3
1492	Q9BPX1	17-beta-hydroxysteroid dehydrogenase 14	6.3507×10^{-5}	0.101946674	5.8	28642	37	1	4.4
998	P60709	actin, cytoplasmic 1	1.5877×10^{-5}	0.102092468	5.29	42052	715	90	34.1
3383	Q9Y5Z4	heme-binding protein 2	1.5877×10^{-5}	0.102129229	4.58	22861	156	3	19.5
964	Q9UNH7	sorting nexin-6	1.5877×10^{-5}	0.102531665	5.81	46905	261	6	15.3
3264	P47756	F-actin-capping protein subunit beta	1.5877×10^{-5}	0.103384254	5.36	31616	265	4	13.7
1609	Q9UL46	proteasome activator complex subunit 2	1.5877×10^{-5}	0.105128204	5.44	27515	94	2	10.9
2914	P21281	V-type proton ATPase subunit B, brain isoform	1.5877×10^{-5}	0.105169042	5.57	56807	509	12	20.5
3305	O00299	chloride intracellular channel protein 1	1.5877×10^{-5}	0.105232399	5.09	27248	262	4	21.2
1548	P06753	tropomyosin alpha-3 chain	1.5877×10^{-5}	0.105267655	4.68	32856	343	36	15.1
1583	P67936	tropomyosin alpha-4 chain	1.5877×10^{-5}	0.106071807	4.67	28619	426	9	30.2
1211	P50213	isocitrate dehydrogenase [NAD] subunit alpha	1.5877×10^{-5}	0.106662107	6.47	40022	150	3	8.5
1581	Q96C19	EF-hand domain-containing protein D2	1.5877×10^{-5}	0.107781812	5.15	26794	46	1	5
2847	Q13885	tubulin beta-2A chain	1.5877×10^{-5}	0.107841883	4.78	50274	319	6	18.9
3311	P62258	14-3-3 protein epsilon	1.5877×10^{-5}	0.108066218	4.63	29326	359	7	27.8
884	Q07960	Rho GTPase-activating protein 1	0.00071446	0.108386461	5.85	50461	291	7	10.9
2556	P14314	glucosidase 2 subunit beta	1.5877×10^{-5}	0.108738059	4.33	60357	194	4	10.2
1457	Q8N8N7	glucosidase 2 subunit beta	1.5877×10^{-5}	0.109312543	5.27	38930	40	1	2.6
2566	P27824	calnexin	1.5877×10^{-5}	0.109775315	4.47	67982	267	6	11.8
1439	P84157	matrix-remodeling-associated protein 7	1.5877×10^{-5}	0.109934952	4.24	21509	172	3	17.6
2180	P04264	keratin, type II cytoskeletal 1	1.5877×10^{-5}	0.110359174	8.15	66170	289	6	11
1247	P06748	nucleophosmin	1.5877×10^{-5}	0.110641094	4.64	32726	42	1	3.1

dx.doi.org/10.1021/pr400929h | J. Proteome Res. XXXX, XXX, XXX–XXX

Table 2. continued

spot no.[a]	accession no.[b]	identified protein	Wilcoxon test p value	fold difference (ratio of means)	pI (cal)[c]	MW (cal) (Da)[c]	protein score[d]	peptide matches	sequence coverage (%)
2214	O75916	regulator of G-protein signaling 9	1.5877×10^{-5}	0.110938705	9.42	77601	36	1	1.2
2612	P08670	vimentin	1.5877×10^{-5}	0.111308534	5.06	53676	1077	24	41.8
2286	Q96QU1	protocadherin-15	1.5877×10^{-5}	0.111433545	4.94	217303	36	1	0.6
1999	P52565	Rho GDP-dissociation inhibitor 1	1.5877×10^{-5}	0.112138698	5.02	23250	216	5	15.2
860	Q9UNH7	sorting nexin-6	1.5877×10^{-5}	0.11235212	5.81	46905	79	2	5.2
1149	P61160	actin-related protein 2	1.5877×10^{-5}	0.112416534	6.3	45017	50	1	3
3513	O60423	probable phospholipid-transporting ATPase IK	1.5877×10^{-5}	0.113222024	7.97	149532	48	1	1.6
1345	Q96JI7	spatacsin	1.5877×10^{-5}	0.113459904	5.63	282621	39	2	1
1814	P61586	transforming protein RhoA	1.5877×10^{-5}	0.113566968	5.83	22096	49	1	4.1
3180	P10809	60 kDa heat shock protein, mitochondrial	1.5877×10^{-5}	0.113616827	5.7	61187	133	3	5.2
533	P29083	general transcription factor IIE subunit 1	1.5877×10^{-5}	0.113756065	4.74	49763	41	1	3.2
3181	Q9UJ70	*N*-acetyl-D-glucosamine kinase	1.5877×10^{-5}	0.114109084	5.81	37694	224	4	14.8
3522	P84077	ADP-ribosylation factor 1	1.5877×10^{-5}	0.114951474	6.32	20741	274	6	32
2952	Q9P1U1	actin-related protein 3B	1.5877×10^{-5}	0.115291654	5.61	48090	76	1	2.6
2254	Q14005	pro-interleukin-16	3.1754×10^{-5}	0.115572204	8.34	142976	41	1	1.3
950	Q01105	protein SET	1.5877×10^{-5}	0.116088182	4.23	33469	278	5	22.8
277	P27824	calnexin	1.5877×10^{-5}	0.117230427	1	67982	584	13	5
1553	P06753	tropomyosin alpha-3 chain	1.5877×10^{-5}	0.117344658	4.68	32856	46	1	3.9
1481	Q49AM3	tetratricopeptide repeat protein 31	1.5877×10^{-5}	0.117497177	8.52	57753	42	1	2.7
1665	P63104	14-3-3 protein zeta/delta	1.5877×10^{-5}	0.119108879	4.73	27899	339	13	24.9
2840	Q13885	tubulin beta-2A chain	1.5877×10^{-5}	0.119125209	4.78	50274	91	2	8.5
498	Q16822	phosphoenolpyruvate carboxykinase [GTP]	1.5877×10^{-5}	0.119425451	7.56	71447	134	3	6.3
3331	Q5TAX3	zinc finger CCHC domain-containing protein 11	1.5877×10^{-5}	0.11952247	8.3	188014	35	1	1
3555	P16949	stathmin	1.5877×10^{-5}	0.119549402	5.76	17292	130	3	20.8
2921	P08670	vimentin	0.00215924	0.120101433	5.06	53676	320	7	14.8
2571	Q9H0J4	glutamine-rich protein 2	1.5877×10^{-5}	0.120540368	6.25	181228	45	1	0.5
3285	P08758	annexin A5	1.5877×10^{-5}	0.120737507	4.94	35971	930	21	48.1
1591	P67936	tropomyosin alpha-4 chain	1.5877×10^{-5}	0.121326925	4.67	28619	165	4	17.3
1433	Q9P1Z9	uncharacterized protein KIAA1529	1.5877×10^{-5}	0.121566905	5.74	192404	44	3	1.2
3452	P09211	glutathione S-transferase P	1.5877×10^{-5}	0.121610737	5.43	23569	205	3	21.4
1840	P51149	Ras-related protein Rab-7a	3.1754×10^{-5}	0.121913756	6.4	23760	171	4	24.6
746	P60709	actin, cytoplasmic 1	1.5877×10^{-5}	0.121964836	5.29	42052	387	11	21.3
2560	P14314	glucosidase 2 subunit beta	1.5877×10^{-5}	0.12226935	4.33	60357	230	4	8.5
1546	Q6ZMW3	echinoderm microtubule-associated protein-like 6	1.5877×10^{-5}	0.124504715	7.17	220270	38	1	0.4
3178	P07951	tropomyosin beta chain	0.00030166	8.436657849	4.66	32945	674	13	34.9
3177	P07951	tropomyosin beta chain	0.00071446	8.672066697	4.66	32945	502	9	27.5
2189	P35030	trypsin-3	0.00730333	8.755681188	7.46	33306	66	1	4.3
3124	P68133	actin, alpha skeletal muscle	0.00409621	13.86346832	5.23	42366	561	16	31.8
3123	P62736	actin, aortic smooth muscle	0.00730333	23.794185	5.23	42381	386	17	19.6

[a]Spot numbers refer to those in Figure 1B. [b]Accession numbers of proteins were derived from Swiss-Plot and NBCI nonredundant databases. [c]Theoretical isoelectric point and molecular weight obtained from Swiss-Prot. [d]Mascot score for the identified proteins based on the peptide ions score ($p < 0.05$) (http://www.matrixscience.com).

Figure 2 in the Supporting Information). We then examined the expression of SET in normal tissues using Western blotting and found that none of these tissues expressed SET (Figure 3C). We surveyed the expression of SET in different histologic types of sarcomas such as gastrointestinal stromal tumor, osteosarcoma, rhabdomyosarcoma, alveolar soft part sarcoma, and epithelioid sarcoma and found that SET was expressed to various degrees in all of them (Figure 3D).

3.3. Functional Verification of the Overexpressed SET Oncogene Product in ASPS Cells

To verify the functional significance of SET overexpression in ASPS, we performed a gene-silencing assay. Transfection of three siRNAs against SET resulted in a marked decrease in SET protein expression (Figure 4A). The cells with reduced SET expression showed significantly diminished cell proliferation relative to cells transfected with control siRNA (Figure 4B). The matrigel invasion assay showed that silencing of SET caused a significant decrease in invasion and migration of ASPS cells (Figure 4C,D). These observations suggested that SET may be involved in tumor progression in ASPS.

3.4. Apoptotic Effects of the PP2A Activator, FTY720, on ASPS Cells

SET is known to be an inhibitor of PP2A, which reduces the kinase-dependent signal transduction pathway, causing

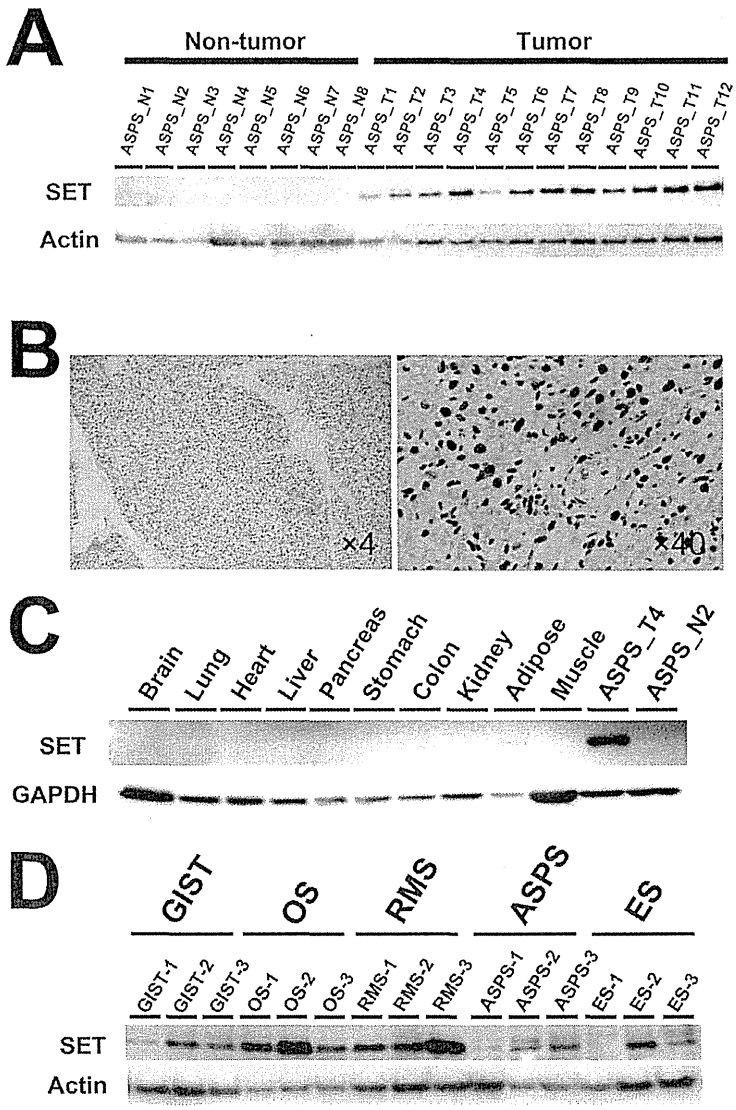

Figure 3. Immunological validation of SET overexpression in ASPS tumor cells. (A) Expression of SET was evaluated in tumor tissues and nontumor tissues by Western blotting. SET was preferentially expressed in tumor tissues. (B) Immunohistochemistry demonstrated the expression and localization of SET in tumor and nontumor tissues. Note that SET was absent in nontumor cells that surrounded tumor cells (left panel). Nuclear localization of SET is demonstrated (right panel). The results of immunohistochemistry for 15 cases of ASPS are exhibited in Supplementary Figure 2 in the Supporting Information. (C) Expression of SET in organs and tissues was evaluated by Western blotting. Note that SET expression was observed only in ASPS tumor tissues. (D) Expression of SET in sarcomas of different histologic types was assessed by Western blotting. Note that SET protein was expressed to various degrees in all of the sarcomas examined.

mitochondria-dependent apoptosis.[20] We hypothesized that the inhibitory effects of SET on PP2A would be responsible for the tumor progression of SET and that the PP2A pathway might be a novel therapeutic target in ASPS. To address this hypothesis, we examined the effects of a PP2A activator, FTY720, on ASPS cells. FTY720 is used for the treatment of patients with multiple sclerosis, and its application to anticancer therapy has been considered.[21] Treatments of ASPS cells with FTY720 markedly suppressed their proliferation in a dose- and time-dependent manner (Figure 5A,B). We found that the PP2A treatment altered the expression of proteins involved in mitochondria-mediated apoptosis, including phosphorylated Akt, Bad, and Bid (Figure 5C), consistent with previous reports.[22−24] These observations suggested the possible utility of the PP2A activator, FTY720, for treatments of ASPS.

4. DISCUSSION

ASPS is refractory to standard chemotherapy and radiation therapy, and novel therapeutic targets have long been sought to improve the clinical outcome.[25] Although proteomics is an approach worth trying for ASPS, no such study has been performed previously, probably because of the extreme rarity of ASPS and the difficulty in obtaining adequate clinical samples. In fact, in 2010, only 11 cases of ASPS were registered in Japan,[26] and gel-based proteomics such as 2D-DIGE requires frozen tissue samples, which are usually not stored in hospitals.

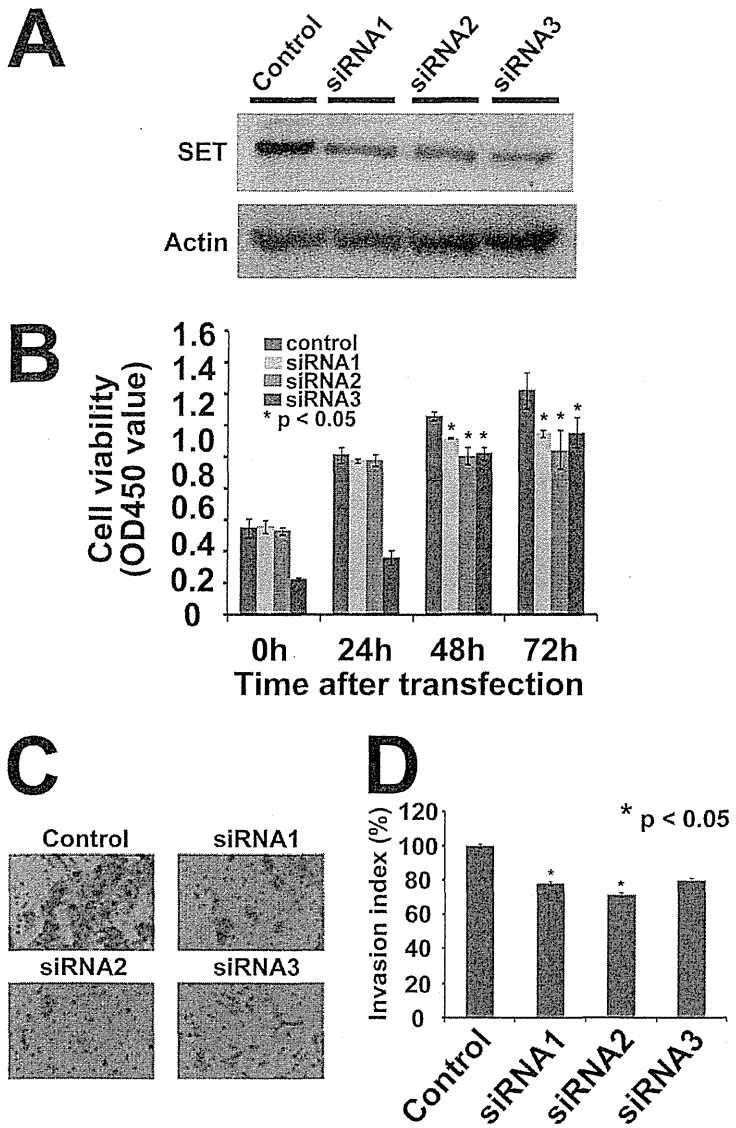

Figure 4. In vitro functional verification of SET in ASPS cells. (A) SET expression was suppressed by treatment with specific siRNAs against SET relative to treatment with control siRNA. Treatment with siRNAs 1–3 decreased the expression of SET in ASPS cells. (B) Proliferation of cells showing decreased SET expression was significantly inhibited. (C) Appearance of invading cells treated with siRNAs against SET. (D) Number of invasive cells was significantly ($p < 0.05$) decreased by treatment with siRNAs 1–3.

These issues are inherent to rare diseases and conventional proteomics methods and are an obstacle to basic research that requires the use of clinical materials. In the present study, we successfully examined 12 samples of frozen ASPS tissue and validated the results of proteomics in 15 cases, including 3 newly enrolled cases (Table 1). Because all cases of ASPS share a common chromosomal rearrangement and expression of an activated transcription factor, ASPL-TFE3,[2] the molecular background of ASPS may be homogeneous. Thus, even from a small number of samples we may be able to obtain results that would shed light on the general background of the disease.

We employed 2D-DIGE to create protein expression profiles. In 2D-DIGE, the proteins are extensively separated according to isoelectric point and molecular weight, and the levels of their expression are evaluated in terms of fluorescent signals, which have a wide dynamic range. Moreover, gel-to-gel variations are compensated for by using a common internal standard sample. We developed our own large-format gel electrophoresis apparatus, which allows wider coverage of the proteome.[27] In the present study, we observed 2300 protein spots, and normalized their intensity (Supplementary Table 2 in the Supporting Information). Together with details of the clinical parameters of the cases employed (Supplementary Table 1 in the Supporting Information), our proteome data will be useful for further studies of ASPS.

We identified higher expression of SET in ASPS tissues relative to adjacent nontumor tissues (Figure 2). Overexpression of SET was confirmed in all 15 cases of ASPS by Western blotting and immunohistochemistry (Figure 2). We found that SET was generally expressed to various degrees in sarcomas (Figure 2). The clinical significance of differences in the expression level

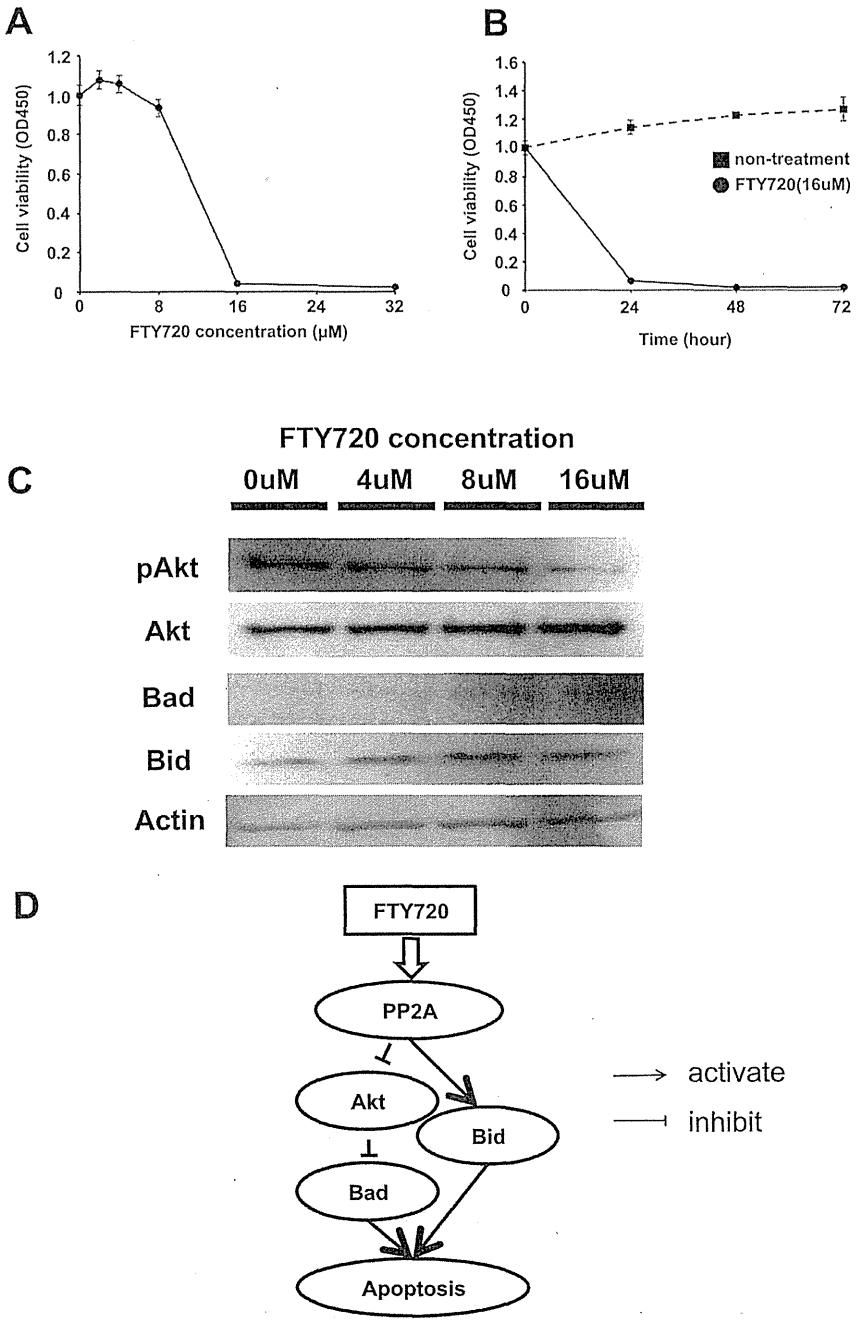

Figure 5. Effects of the PP2A activator, FTY720, on cell proliferation and apoptosis. (A) Effects of FTY720 on cell viability were examined as a function of FTY720concentration. (B) Time-dependent inhibitory effects of FTY720 (16 μM) on cell viability. (C) Effects of FTY720 at various concentrations on the expression of apoptosis-regulating proteins were examined by Western blotting. Note that treatment of the cells with FTY720 caused a reduction in the expression of pAkt and increased the expression of Bad and Bid. In contrast, Akt expression level was not affected by FTY720 treatments. These proteins were not observed by 2D-DIGE. (D) Activation of PP2A by treatment with FTY720 triggers the apoptosis pathway, resulting in reduced proliferation of ASPS cells.

of SET may be worth investigating in the context of its predictive or prognostic utility. In this study, the SET expression was observed in ASPS and the other sarcomas but not in normal tissues examined, suggesting that SET expression may represent common characters of malignancies including sarcomas.

The molecular mechanisms responsible for SET overexpression are intriguing but still unclear. ASPS is characterized by chromosomal rearrangement and expression of an activated transcription factor, ASPL-TFE3.[2] Genes under the control of this fusion gene have been revealed by DNA microarray experiments, and such genes would likely account for the molecular

background of hyper-angiogenesis observed in ASPS.[3−5] However, SET is not one of the genes that are regulated by ASPL-TFE3.[3−5] Cervoni et al. reported overexpression of SET in various cancers such as those of the breast, uterus, colorectum, stomach, and kidney relative to their adjacent normal tissues[28] but not in ASPS. Recently, in a study of chronic myeloid leukemia, Piazza et al. found a mutation in SET binding protein 1 (SETBP1), which hindered the degradation of SET and increased the expression level of both SETBPs and SET.[29] Elucidation of the functional properties of the protein complex of SET may provide further insight into the etiology of ASPS. Because higher expression of SET is observed in a wide variety of malignancies, it may be attributable to common and important molecular mechanisms and therefore warrants further investigation. It is interesting if SET is a key to reach to common molecular backgrounds among malignancies including ASPS.

Because overexpression of SET may be a novel therapeutic target in ASPS, we focused on SET in the present study. SET is a multifunctional protein with an inhibitory effect on the activity of PP2A, which is one of the major cellular serine-threonine phosphatases[21] and negatively regulates signaling pathways such as the PI3K/Akt pathway,[30] which is aberrantly regulated in various cancers. PP2A is a tumor-suppressor protein, and its functional inactivation has been reported in several cancers.[31] Switzer et al. have reported a novel SET interactive peptide, COG112, which inhibits the association between SET and the PP2A catalytic subunit.[32] Treatment of cancer cells with CIG112 increases PP2A activity and inhibits Akt signaling and cellular proliferation. In leukemia, activators of PP2A such as forskolin,[33] 1,9-dideoxy-forskolin,[34] and FTY720[35] effectively antagonize leukemogenesis. Remarkably, even in imatinib-resistant leukemia cells, restoration of PP2A activity, either by application of a chemical PP2A activator or interference with SET/PP2A interplay, has been reported to inactivate BCR/ABL, trigger growth suppression, enhance apoptosis, and impair leukemogenesis.[36] Therefore, PP2A may be a promising drugable therapeutic target for patients who show resistance to treatment. In rare diseases, it may be difficult to develop original drugs because of their low commercial potential; therefore, additional use of existing drugs may be regarded as a more practical approach. Here we focused on FTY720 because it has been used for treatment of multiple sclerosis and malignancies.[21] We found that treatment of ASPS cells with FTY720 induced apoptosis and inhibited cell proliferation, invasion, and migration (Figure 3). ASPS exhibits MET autophosphorylation following activation of downstream signaling pathways, and the clinical efficacy of a multikinase inhibitor, sunitinib malate, has been demonstrated in ASPS.[12,13,37] Because FTY720 affects the signal transduction pathway through a mechanism differing from than of MET, it would be worth examining the utility of PP2A activator for ASPS patients who show resistance to kinase inhibitors. The effects of FTY720 on ASPS cells should be investigated further using additional cell lines and animal models.

In conclusion, we have successfully identified the expression of SET in ASPS using a proteomics approach. The possible application of PP2A activator for treatment of ASPS will be investigated further. Because overexpression of SET was generally observed in sarcomas, the application of the PP2A activators for sarcoma treatments is worth examining. To elucidate the molecular background responsible for overexpression of SET, it is essential to establish ASPS cell lines. We anticipate that our research activity will eventually be of benefit to ASPS patients.

■ ASSOCIATED CONTENT

Supporting Information

Supplementary Figure 1: Typical image of two-dimensional difference gel electrophoresis. Supplementary Figure 2: Immunohistochemistry of SET in tumor cells and non-tumor cells. Supplement Table 1: Patient's characteristics of various saroma cases Supplement Table 2: A summary of the intensity of all protein spots. Supplement Table 3: Supportive information for protein identification. This material is available free of charge via the Internet at http://pubs.acs.org.

■ AUTHOR INFORMATION

Corresponding Author

*Tel: +81-3-3542-2511. Fax: +81-3-3547-5298. E-mail: takondo@ncc.go.jp.

Notes

The authors declare no competing financial interest.

■ ACKNOWLEDGMENTS

This study was supported by the National Cancer Center Research Core Facility and by the National Cancer Center Research and Development Fund (23-A-7 and 23-A-10). Patient's characteristics of various saroma cases.

■ REFERENCES

(1) Christopherson, W. M.; Foote, F. W., Jr.; Stewart, F. W. Alveolar soft-part sarcomas; structurally characteristic tumors of uncertain histogenesis. *Cancer* **1952**, *5* (1), 100−111.

(2) Ladanyi, M.; Lui, M. Y.; Antonescu, C. R.; Krause-Boehm, A.; Meindl, A.; Argani, P.; Healey, J. H.; Ueda, T.; Yoshikawa, H.; Meloni-Ehrig, A.; Sorensen, P. H.; Mertens, F.; Mandahl, N.; van den Berghe, H.; Sciot, R.; Dal Cin, P.; Bridge, J. The der(17)t(X;17)(p11;q25) of human alveolar soft part sarcoma fuses the TFE3 transcription factor gene to ASPL, a novel gene at 17q25. *Oncogene* **2001**, *20* (1), 48−57.

(3) Lazar, A. J.; Das, P.; Tuvin, D.; Korchin, B.; Zhu, Q.; Jin, Z.; Warneke, C. L.; Zhang, P. S.; Hernandez, V.; Lopez-Terrada, D.; Pisters, P. W.; Pollock, R. E.; Lev, D. Angiogenesis-promoting gene patterns in alveolar soft part sarcoma. *Clin. Cancer Res.* **2007**, *13* (24), 7314−7321.

(4) Stockwin, L. H.; Vistica, D. T.; Kenney, S.; Schrump, D. S.; Butcher, D. O.; Raffeld, M.; Shoemaker, R. H. Gene expression profiling of alveolar soft-part sarcoma (ASPS). *BMC Cancer* **2009**, *9*, 22.

(5) Covell, D. G.; Wallqvist, A.; Kenney, S.; Vistica, D. T. Bioinformatic analysis of patient-derived ASPS gene expressions and ASPL-TFE3 fusion transcript levels identify potential therapeutic targets. *PLoS One* **2012**, *7* (11), e48023.

(6) Bisogno, G.; Rosolen, A.; Carli, M. Interferon alpha for alveolar soft part sarcoma. *Pediatr. Blood Cancer* **2005**, *44* (7), 687−688.

(7) Roozendaal, K. J.; de Valk, B.; ten Velden, J. J.; van der Woude, H. J.; Kroon, B. B. Alveolar soft-part sarcoma responding to interferon alpha-2b. *Br. J. Cancer* **2003**, *89* (2), 243−245.

(8) Kuriyama, K.; Todo, S.; Hibi, S.; Morimoto, A.; Imashuku, S. Alveolar soft part sarcoma with lung metastases. Response to interferon alpha-2a? *Med. Pediatr. Oncol.* **2001**, *37* (5), 482−483.

(9) Azizi, A. A.; Haberler, C.; Czech, T.; Gupper, A.; Prayer, D.; Breitschopf, H.; Acker, T.; Slavc, I. Vascular-endothelial-growth-factor (VEGF) expression and possible response to angiogenesis inhibitor bevacizumab in metastatic alveolar soft part sarcoma. *Lancet Oncol.* **2006**, *7* (6), 521−523.

(10) Mir, O.; Boudou-Rouquette, P.; Larousserie, F.; Blanchet, B.; Babinet, A.; Anract, P.; Goldwasser, F. Durable clinical activity of single-agent bevacizumab in a nonagenarian patient with metastatic alveolar soft part sarcoma. *Anticancer Drugs* **2012**, *23* (7), 745−748.

(11) Demetri, G. D.; van Oosterom, A. T.; Garrett, C. R.; Blackstein, M. E.; Shah, M. H.; Verweij, J.; McArthur, G.; Judson, I. R.; Heinrich, M. C.; Morgan, J. A.; Desai, J.; Fletcher, C. D.; George, S.; Bello, C. L.;

Huang, X.; Baum, C. M.; Casali, P. G. Efficacy and safety of sunitinib in patients with advanced gastrointestinal stromal tumour after failure of imatinib: a randomised controlled trial. *Lancet* **2006**, *368* (9544), 1329–1338.

(12) Stacchiotti, S.; Tamborini, E.; Marrari, A.; Brich, S.; Rota, S. A.; Orsenigo, M.; Crippa, F.; Morosi, C.; Gronchi, A.; Pierotti, M. A.; Casali, P. G.; Pilotti, S. Response to sunitinib malate in advanced alveolar soft part sarcoma. *Clin. Cancer Res.* **2009**, *15* (3), 1096–1104.

(13) Stacchiotti, S.; Negri, T.; Zaffaroni, N.; Palassini, E.; Morosi, C.; Brich, S.; Conca, E.; Bozzi, F.; Cassinelli, G.; Gronchi, A.; Casali, P. G.; Pilotti, S. Sunitinib in advanced alveolar soft part sarcoma: evidence of a direct antitumor effect. *Ann. Oncol.* **2011**, *22* (7), 1682–1690.

(14) Hanash, S. Progress in mining the human proteome for disease applications. *OMICS* **2011**, *15* (3), 133–139.

(15) Balgley, B. M.; Guo, T.; Zhao, K.; Fang, X.; Tavassoli, F. A.; Lee, C. S. Evaluation of archival time on shotgun proteomics of formalin-fixed and paraffin-embedded tissues. *J. Proteome Res.* **2009**, *8* (2), 917–925.

(16) von Lindern, M.; van Baal, S.; Wiegant, J.; Raap, A.; Hagemeijer, A.; Grosveld, G. Can, a putative oncogene associated with myeloid leukemogenesis, may be activated by fusion of its 3′ half to different genes: characterization of the set gene. *Mol. Cell. Biol.* **1992**, *12* (8), 3346–3355.

(17) Li, M.; Makkinje, A.; Damuni, Z. The myeloid leukemia-associated protein SET is a potent inhibitor of protein phosphatase 2A. *J. Biol. Chem.* **1996**, *271* (19), 11059–11062.

(18) Seshacharyulu, P.; Pandey, P.; Datta, K.; Batra, S. K. Phosphatase: PP2A structural importance, regulation and its aberrant expression in cancer. *Cancer Lett.* **2013**, *335* (1), 9–18.

(19) Kondo, T.; Hirohashi, S. Application of highly sensitive fluorescent dyes (CyDye DIGE Fluor saturation dyes) to laser microdissection and two-dimensional difference gel electrophoresis (2D-DIGE) for cancer proteomics. *Nat. Protoc.* **2006**, *1* (6), 2940–2956.

(20) Perrotti, D.; Neviani, P. Protein phosphatase 2A: a target for anticancer therapy. *Lancet Oncol.* **2013**, *14* (6), e229–e238.

(21) Perrotti, D.; Neviani, P. Protein phosphatase 2A (PP2A), a drugable tumor suppressor in Ph1(+) leukemias. *Cancer Metastasis Rev.* **2008**, *27* (2), 159–168.

(22) Yasui, H.; Hideshima, T.; Raje, N.; Roccaro, A. M.; Shiraishi, N.; Kumar, S.; Hamasaki, M.; Ishitsuka, K.; Tai, Y. T.; Podar, K.; Catley, L.; Mitsiades, C. S.; Richardson, P. G.; Albert, R.; Brinkmann, V.; Chauhan, D.; Anderson, K. C. FTY720 induces apoptosis in multiple myeloma cells and overcomes drug resistance. *Cancer Res.* **2005**, *65* (16), 7478–7484.

(23) Nagahara, Y.; Ikekita, M.; Shinomiya, T. T cell selective apoptosis by a novel immunosuppressant, FTY720, is closely regulated with Bcl-2. *Br. J. Pharmacol.* **2002**, *137* (7), 953–962.

(24) Matsumura, M.; Tsuchida, M.; Isoyama, N.; Takai, K.; Matsuyama, H. FTY720 mediates cytochrome c release from mitochondria during rat thymocyte apoptosis. *Transpl. Immunol.* **2010**, *23* (4), 174–179.

(25) Kayton, M. L.; Meyers, P.; Wexler, L. H.; Gerald, W. L.; LaQuaglia, M. P. Clinical presentation, treatment, and outcome of alveolar soft part sarcoma in children, adolescents, and young adults. *J. Pediatr. Surg.* **2006**, *41* (1), 187–193.

(26) *Soft Tissue Tumor Registry in Japan*, 2010.

(27) Kondo, T.; Hirohashi, S. Application of highly sensitive fluorescent dyes (CyDye DIGE Fluor saturation dyes) to laser microdissection and two-dimensional difference gel electrophoresis (2D-DIGE) for cancer proteomics. *Nat. Protoc.* **2007**, *1* (6), 2940–2956.

(28) Cervoni, N.; Detich, N.; Seo, S. B.; Chakravarti, D.; Szyf, M. The oncoprotein Set/TAF-1beta, an inhibitor of histone acetyltransferase, inhibits active demethylation of DNA, integrating DNA methylation and transcriptional silencing. *J. Biol. Chem.* **2002**, *277* (28), 25026–25031.

(29) Piazza, R.; Valletta, S.; Winkelmann, N.; Redaelli, S.; Spinelli, R.; Pirola, A.; Antolini, L.; Mologni, L.; Donadoni, C.; Papaemmanuil, E.; Schnittger, S.; Kim, D. W.; Boultwood, J.; Rossi, F.; Gaipa, G.; De Martini, G. P.; di Celle, P. F.; Jang, H. G.; Fantin, V.; Bignell, G. R.; Magistroni, V.; Haferlach, T.; Pogliani, E. M.; Campbell, P. J.; Chase, A. J.; Tapper, W. J.; Cross, N. C.; Gambacorti-Passerini, C. Recurrent SETBP1 mutations in atypical chronic myeloid leukemia. *Nat. Genet.* **2013**, *45* (1), 18–24.

(30) Ivaska, J.; Nissinen, L.; Immonen, N.; Eriksson, J. E.; Kahari, V. M.; Heino, J. Integrin alpha 2 beta 1 promotes activation of protein phosphatase 2A and dephosphorylation of Akt and glycogen synthase kinase 3 beta. *Mol. Cell. Biol.* **2002**, *22* (5), 1352–1359.

(31) Janssens, V.; Goris, J.; Van Hoof, C. PP2A: the expected tumor suppressor. *Curr. Opin. Genet. Dev.* **2005**, *15* (1), 34–41.

(32) Switzer, C. H.; Cheng, R. Y.; Vitek, T. M.; Christensen, D. J.; Wink, D. A.; Vitek, M. P. Targeting SET/I(2)PP2A oncoprotein functions as a multi-pathway strategy for cancer therapy. *Oncogene* **2011**, *30* (22), 2504–2513.

(33) Feschenko, M. S.; Stevenson, E.; Nairn, A. C.; Sweadner, K. J. A novel cAMP-stimulated pathway in protein phosphatase 2A activation. *J Pharmacol. Exp. Ther.* **2002**, *302* (1), 111–118.

(34) Neviani, P.; Santhanam, R.; Trotta, R.; Notari, M.; Blaser, B. W.; Liu, S.; Mao, H.; Chang, J. S.; Galietta, A.; Uttam, A.; Roy, D. C.; Valtieri, M.; Bruner-Klisovic, R.; Caligiuri, M. A.; Bloomfield, C. D.; Marcucci, G.; Perrotti, D. The tumor suppressor PP2A is functionally inactivated in blast crisis CML through the inhibitory activity of the BCR/ABL-regulated SET protein. *Cancer Cell* **2005**, *8* (5), 355–368.

(35) Matsuoka, Y.; Nagahara, Y.; Ikekita, M.; Shinomiya, T. A novel immunosuppressive agent FTY720 induced Akt dephosphorylation in leukemia cells. *Br. J. Pharmacol.* **2003**, *138* (7), 1303–1312.

(36) Perrotti, D.; Neviani, P. ReSETting PP2A tumour suppressor activity in blast crisis and imatinib-resistant chronic myelogenous leukaemia. *Br. J. Cancer* **2006**, *95* (7), 775–781.

(37) George, S.; Merriam, P.; Maki, R. G.; Van den Abbeele, A. D.; Yap, J. T.; Akhurst, T.; Harmon, D. C.; Bhuchar, G.; O'Mara, M. M.; D'Adamo, D. R.; Morgan, J.; Schwartz, G. K.; Wagner, A. J.; Butrynski, J. E.; Demetri, G. D.; Keohan, M. L. Multicenter phase II trial of sunitinib in the treatment of nongastrointestinal stromal tumor sarcomas. *J. Clin. Oncol* **2009**, *27* (19), 3154–3160.

Published in final edited form as:
Protoc exch. ; 2014: .

A novel approach to pseudopodia proteomics: excimer laser etching, two-dimensional difference gel electrophoresis, and confocal imaging

Takahiro Mimae[1,2,3,7], **Akihiko Ito**[2,4,7], **Man Hagiyama**[2,4], **Jun Nakanishi**[5], **Yoichiroh Hosokawa**[6], **Morihito Okada**[1], **Yoshinori Murakami**[2], and **Tadashi Kondo**[3]

[1]Department of Surgical Oncology, Research Institute for Radiation Biology and Medicine, Hiroshima University, Hiroshima 734-8511, Japan

[2]Division of Molecular Pathology, Department of Cancer Biology, Institute of Medical Science, University of Tokyo, Tokyo 108-8639, Japan

[3]Division of Pharmacoproteomics, National Cancer Center Research Institute, Tokyo 104-0045, Japan

[4]Department of Pathology, Faculty of Medicine, Kinki University, Osaka 589-8511, Japan

[5]Nidek Co. Ltd., Gamagori, Aichi 443-0038, Japan

[6]Nara Institute of Science and Technology, Ikoma, Nara 630-0192, Japan

Abstract

Pseudopodia are actin-rich ventral cellular protrusions shown to facilitate the migration and metastasis of tumor cells. Here, we present a novel approach to perform pseudopodia proteomics. Tumor cells growing on porous membranes extend pseudopodia into the membrane pores. In our method, cell bodies are removed by horizontal ablation at the basal cell surface with the excimer laser while pseudopodia are left in the membrane pores. For protein expression profiling, whole cell and pseudopodia proteins are extracted with a lysis buffer, labeled with highly sensitive fluorescent dyes, and separated by two-dimensional gel electrophoresis. Proteins with unique expression patterns in pseudopodia are identified by mass spectrometry. The effects of the identified proteins on pseudopodia formation are evaluated by measuring the pseudopodia length in cancer cells with genetically modified expression of target proteins using confocal imaging. This protocol allows global identification of pseudopodia proteins and evaluation of their functional significance in pseudopodia formation within one month.

Correspondence should be addressed to: Tadashi Kondo, MD, PhD, Division of Pharmacoproteomics, National Cancer Center Research Institute, 5-1-1 Tsukiji, Chuo-ku, Tokyo 104-0045, Japan, Tel: 81-3-3542-2511 ext.3004, Fax: 81-3-3547-5298, takondo@ncc.go.jp.
[7]These authors contributed equally to this work.

Disclosure/Duality of Interest
The authors declare no conflict of interest.

Supporting Information
Supplementary Information can be found on the *Laboratory Investigation* website (http://www.laboratoryinvestigation.org)

Keywords

pseudopodia; proteomics; excimer laser ablation; two-dimensional difference gel electrophoresis; confocal imaging

1. Introduction: pseudopodia proteomics in cancer invasion research

Pseudopodia are dynamic, actin-rich cellular protrusions essential for cell and tissue motility. The polarized formation of pseudopodial protrusions during cell migration plays a critical role in a variety of physiological and pathological processes including cancer metastasis[1–3]. Many lines of evidence have suggested that many cancer-associated proteins are involved in pseudopodia formation, promoting invasive migration of tumor cells. Pseudopodial actin-rich structures, which play a central role in pseudopodia functions, are aberrantly regulated in various cancers[4]. Protein kinases such as focal adhesion kinase and Src kinase were found to be enriched in pseudopodial protrusions, and various phosphorylated proteins were observed in pseudopodia[5,6]. Glycolytic enzymes colocalized with pseudopodial actin structures may supply energy for the formation of pseudopodial protrusions and promote motility of tumor cells[7]. Cancer-associated cytokines stimulate intracellular signaling pathways and subsequently facilitate actin reorganization and pseudopodial protrusions[8,9]. Epithelial to mesenchymal transition, a critical process in cancer cell invasion and metastasis, is regulated by pseudopodial proteins[10]. These observations indicate that a variety of unique proteins are involved in pseudopodia formation and function in a cooperative manner. Therefore, the identification of pseudopodia-specific proteins using global protein expression profiling methods such as pseudopodia proteomics will reveal the mechanisms underlying tumor cell invasion and migration. Moreover, as the disruption of pseudopodia formation suppresses metastasis of tumor cells, the identification of pseudopodia-specific proteins may lead to the development of novel approaches to cancer therapy[1–3].

2. Technical challenges in pseudopodia proteomics

In the model system of pseudopodia formation, cells are plated on a porous membrane positioned over conditioned chemoattractant-containing medium and allowed to extend pseudopodia through the membrane pores (Figure 1)[7]. As pseudopodia are a rich source of metastasis-associated proteins, pseudopodia proteomics is an attractive approach to investigate cancer biology. Although several studies have reported global protein composition of pseudopodia and a number of intriguing proteins have been identified, there are still many technical challenges in pseudopodia proteomics. Pseudopodia proteomics involves three major steps: pseudopodia purification, protein expression profiling, and functional evaluation of the identified pseudopodia-specific proteins. All these steps have inherent limitations that compromise the current approach to pseudopodia proteomics.

First, pseudopodia should be separated from a cell body without damage to their structure. In the previous studies, for the isolation of pseudopodia, cells were seeded on a porous membrane, and cell bodies were manually wiped off the top of the membrane with a cotton-tipped swab. Subsequently, proteins were extracted from the membrane containing

pseudopodial protrusions and subjected to protein expression profiling[5,11,12]. Although this approach has led to the identification of a considerable number of pseudopodia-associated proteins, the manual isolation of pseudopodia may potentially cause contamination with cell body proteins; in addition, pseudopodia may be mechanically damaged during isolation by an operator. As the protein amount in a cell body exceeds that in a pseudopodium by more than ten times, cell bodies have to be completely removed from the membrane in the process of pseudopodia isolation. On the other hand, stringent wiping of cell bodies with a cotton swab may result in the loss of functionally important pseudopodia proteins with low expression levels. Thus, a novel approach is needed for the precise isolation of intact pseudopodia from cell bodies in a controlled, operator-independent manner.

Second, pseudopodia proteomics analysis should be conducted in a quantitative way. Pseudopodia-specific proteins are identified by the comparison between the protein expression profiles in cell bodies and pseudopodia. As some proteins may be present both in the cell body and pseudopodia but expressed at different levels, pseudopodia proteomics should be performed in a more directly quantitative manner. Previous studies have used mass spectrometry to identify pseudopodia proteins; however, although a number of pseudopodial proteins have been described with this method, the protein expression patterns in pseudopodia and cell bodies were not quantitatively evaluated[5]. For example, using mass spectrometry, Shankar et al. compared the protein contents in pseudopodia and cell bodies; but not the protein expression profiles[10]. Quantitative comparison was achieved by using the isotope-labeling method. Wang et al. applied the $^{16}O/^{18}O$ labeling method to compare cell body and pseudopodia protein expression[12]. In this method, the proteins of two samples were digested with trypsin and labeled separately with ^{16}O and ^{18}O, which were incorporated into peptide carboxyl groups in a sequence-independent manner. The samples were mixed, and the relative abundance of ^{16}O-labeled and ^{18}O-labeled peptides was evaluated by mass spectrometry. The $^{16}O/^{18}O$ labeling method has enabled precise comparison of thousands of peptides in small samples; however, the linear dynamic range of detection in mass spectrometry is limited to 10^2–10^3 [13]. Considering that the dynamic range of protein expression reaches 10^{11}, this method is not optimal for pseudopodia proteomics. As an alternative to mass spectrometry, the gel-based approach coupled with fluorescent labeling, such as two-dimensional difference gel electrophoresis (2D-DIGE), has been for pseudopodia proteomics[14,15]. However, as the sensitivity of fluorescence detection in these studies was equivalent to that of silver staining, large protein amounts, from 50 to 170 μg[14,15], were required for protein expression profiling. As the amount of pseudopodia proteins is quite limited, a more sensitive method is needed to avoid laborious pseudopodia isolation and possible protein degradation. Proteomic modalities with a wide dynamic range and high sensitivity are required for pseudopodia protein profiling.

Third, the biological properties of pseudopodial proteins identified by proteomics should be functionally verified by observing the effects on pseudopodia formation and elongation. In a previous study, the number of newly generated pseudopodia and the extent of extracellular matrix degradation were evaluated as parameters of tumor cell invasive potential[16]. In addition to newly generated pseudopodia, the effects on existing pseudopodia should also be assessed in a quantitative way.

3. A novel approach to pseudopodia proteomics

To address the above-mentioned issues, we developed a novel approach to pseudopodia proteomics. Our systematic approach consists of three steps: isolation of pseudopodia from cell bodies by laser ablation, protein expression profiling using small amounts of pseudopodia protein extracts and highly sensitive fluorescent dyes, and functional evaluation of the newly identified pseudopodia proteins using confocal imaging.

3.1. Isolation of pseudopodia from cell bodies by excimer laser etching

To isolate pseudopodia of tumor cells, we applied a medical device used for laser-assisted *in situ* keratomileusis (LASIK), a procedure in ophthalmic refractive surgery. In LASIK, superficial anterior corneal tissue is reshaped by a topographically assisted excimer laser after the epithelium is flapped from the Bowman's layer (Figure 1)[17]. Surgical complications rarely occur in LASIK because the excimer laser ablates living tissues in a precisely horizontal manner without thermal damage to the underlying tissue layers[18]. In our method, cell ablation at the ventral level with the excimer laser completely removed cell bodies from the porous membrane, and the pseudopodia structures, which remained intact inside the pores, were treated with protein extraction buffer for subsequent protein expression profiling. The laser ablation was performed in an operator-independent manner.

The excimer laser-assisted cell etching technique allows the ablation of cell bodies without damaging pseudopodia in the pores. The idea is based on spatial parameters of the laser-cell interaction. In our experiments, the laser keratectomy system was equipped with an argon fluoride excimer laser with a wavelength of 193 nm. Peptide bonds (O=C–N–N) in the protein backbone absorb laser energy; at this wavelength, the optical tissue penetration depth is approximately 500 nm[19]. Therefore, possible protein degradation would be induced only within 500 nm from the pseudopodium base. Moreover, the membrane pore diameter (1–3 μm) exceeds the laser wavelength by 15 times; therefore, at 193 nm the membrane may exhibit a strong light-scattering effect. Thus, because of the ratio between the laser wavelength and pore size, the excimer laser pulses do not reach pseudopodia in the pores. We have demonstrated that there was no protein degradation in the isolated pseudopodia based on light microscopy and immunoblotting observations[20].

3.2. 2D-polyacrylamide gel electrophoresis (PAGE) with highly sensitive fluorescent dyes for the separation of a small amount of pseudopodia proteins

To create quantitative protein expression profiles using a very small amount of proteins recovered from the isolated pseudopodia, we labeled the proteins with a highly sensitive fluorescent dye and separated them using 2D-DIGE. Two types of fluorescent dyes are available for 2D-DIGE, Cy3 and Cy5[21,22], and the dyes with higher sensitivity have been used for pseudopodia proteomics [22].

Protein separation based on 2D-PAGE enables the quantitative comparative analysis of thousands of proteins and has been used in a variety of research applications. In a classical 2D-PAGE analysis, proteins are separated according to their isoelectric point and molecular weight and identified using colorimetric detection such as silver staining; protein expression

is then evaluated based on relative staining intensity. The drawback of using 2D-PAGE with silver staining is its narrow linear dynamic range of protein detection (10^3)[23], which hampers quantitative comparison, as is the case with mass spectrometry. According to our previous findings, 2D-PAGE coupled with silver staining required cell material from more than five sheets of porous membranes[20]. Thus, although 2D-PAGE is one of the candidate modalities for pseudopodia proteomics, silver staining is not practically suitable for the detection of pseudopodial proteins.

In 2D-DIGE, proteins in different samples are labeled with individual fluorescent dyes and resolved by 2D-PAGE; the separated proteins are detected by fluorescence using a laser scanner. As multiple protein samples are simultaneously separated in identical gels, gel-to-gel variations can be compensated. Moreover, protein spot intensities are measured as fluorescent signals with a wide linear dynamic range of 10^5; therefore, a reliable quantitative comparison between samples can be achieved. We developed a novel method to label laser-microdissected tissues using highly sensitive fluorescent dyes (CyDye DIGE Fluor saturation dyes) and reported that only 3000 cells were required to generate protein expression profiles[24,25]. In a previous study, 2D-DIGE was also applied to examination of pseudopodia proteins obtained through a conventional cotton-puff wiping procedure[14]; however, the sensitivity of a home-made fluorescent dye used in that study was equivalent to that of silver staining, and only highly abundant species such as heat shock and cytoskeletal proteins were detected. In our experiments, we used CyDye DIGE Fluor saturation dyes, which enabled the expression profiling using small amounts of pseudopodia proteins.

In our previous experiments, protein identification was achieved by mass spectrometry using high amounts of whole cell proteins separated in a preparative gel[24]. By using 2D-DIGE and a sensitive fluorescent dye, global protein profiling can be performed using only a few micrograms of protein; however, the protein amount in gel spots does not reach the sensitivity of mass spectrometry. Therefore, target protein spots are detected in the preparative gel using the image analysis software and recovered for protein identification.

3.3. Functional analysis of pseudopodia proteins using confocal imaging

To investigate the functions of the identified proteins in pseudopodia formation, we developed a novel imaging system based on immunocytochemistry and confocal microscopy. In our method, the transient overexpression or silencing of the identified proteins were achieved by transfection with expression vectors or specific siRNA, respectively. The protein localization and the status of pseudopodia are monitored by confocal imaging. The effects of transfection on the pseudopodia formations are quantitatively evaluated by measuring the pseudopodia length and the number of protrusions, and pseudopodia functional activity was assessed based on cell motility and invasiveness[20,26]. The elongation of pseudopodia protrusions is an important step in cell movement and invasion[27], and the cells with elongated protrusions may be potentially more invasive than those with shorter pseudopodia.

4. Limitations of the pseudopodia proteomic approach based on combination of excimer laser etching, 2D-DIGE, and confocal imaging

To isolate pseudopodia, we used a sophisticated and rather expensive medical device specifically developed for ophthalmic refractive surgery, which was approved by the relevant institutions. Although the device has demonstrated excellent performance in isolation of pseudopodia, its high cost dictates the necessity to develop a simple and less expensive device for basic experiments.

Another limitation of our novel approach is the chemoattractant-containing media. In our protocols, we used NIH3T3-conditioned medium, which induced MDA-MB-231 and MCF-7 human breast cancer cells and B16-F10 murine melanoma cells plated on fibronectin-coated porous membranes to sprout out the protrusions into the pores. However, this medium did not promote the formation of pseudopodia in SBC-3 and SBC-5 human small cell lung cancer cells or MSTO-211H human mesothelioma cells, indicating that cell-specific chemoattractants should be used.

In our previous study, approximately 100 unique pseudopodia proteins were identified using the combination of the excimer laser etching technique and 2D-DIGE[20]. However, they did not include some of the well-established pseudopodia proteins, such as integrin beta, indicating that the actual number of pseudopodia-specific proteins may be higher. In this study, we detected approximately 50 proteins with acidic isoelectric points. According to the genome information, acidic and basic proteins exist in the cell in approximately equal numbers. Assuming the same proportion among the pseudopodia proteins, we may be able to observe some 50 species in the alkaline range. Gorg et al. reported that the use of isoelectric focusing gels with a narrow isoelectric point range resulted in the detection of low-abundance proteins[28]. Fractionation of pseudopodia proteins prior to 2D-DIGE may be a potential solution to overcome this problem; however, possible protein loss during fractionation may occur.

In our method, the functions of pseudopodia proteins were evaluated by genetically regulating target protein expression and assessing the changes in pseudopodia behavior using confocal imaging. However, the length of pseudopodia does not fully reflect their functional activity. Our method can be considered as the first step of functional evaluation, and a multi-faceted approach may be required to better understand the regulatory effects of pseudopodial proteins[16].

5. Applications

The combination of the excimer laser etching technique, 2D-DIGE, and confocal imaging is applicable to proteomic studies of membrane ventral protrusions, including pseudopodia and invadopodia, in any adherent cancer cell type. Proteins differentially expressed in membrane protrusions may contribute to understanding of the invasion and metastasis of tumor cells, and our method will provide further understanding of the malignant cancer phenotype.

MATERIALS

REAGENTS

Penicillin-streptomycin, liquid (Invitrogen; Carlsbad, CA, USA; cat. no. 15070-063).

Culture plates with 12 wells (BD; Franklin Lakes, NJ, USA; cat. no. 353043).

Dulbecco's modified Eagle medium (DMEM) (NakalaiTesque; Kyoto, Japan; cat. no. 14247-15).

Fetal bovine serum (FBS) (Biological Industries; Israel; cat. no. 04-001-1A).

Human fibronectin (Sigma-Aldrich; St. Louis, MO; USA; cat. no. F0895).

L-glutamine (Sigma-Aldrich; cat. no. G7513) GlutaMAX (GIBCO; Carlsbad, CA, USA; cat. no. 35050-061).

L-15 (Sigma-Aldrich; Gillingham, UK; cat. no. L5520).

Dulbecco's phosphate-buffered saline (D-PBS) (Wako; Japan; cat. no. 045-29795).

Formaldehyde (Wako; cat. no. 064-00406).

! CAUTION Formaldehyde is flammable and toxic by skin contact. Wear gloves when handling.

Mayer's hematoxylin solution (Muto Pure Chemicals; Tokyo, Japan; cat. no.3000-2).

! CAUTION Hematoxylin is flammable and toxic by skin contact. Wear gloves when handling.

Eosin alcohol solution, 0.5% (Muto Pure Chemicals).

! CAUTION Eosin is flammable and toxic by skin contact. Wear gloves when handling.

Xylene (Wako; cat. no. 244-00086).

! CAUTION Xylene is flammable and toxic by skin contact. Wear gloves when handling.

Mounting reagent (O. Kindler; Freiburg; Germany).

Urea, EP-MB grade (Roche Diagnostics; Mannheim, Germany; cat. no. 11685899001).

Thiourea (Sigma-Aldrich; cat. no. T7875).

CHAPS (Wako; cat. no. 345-04724).

Triton X-100 (GE Healthcare Biosciences, NJ; USA; cat. no. 17-1315-01).

Dithiothreitol (DTT) (Wako; cat. no. 049-08972).

Pharmalyte, pH 3–10 (GE Healthcare Biosciences; cat. no. 17-0456-01).

CyDye DIGE Fluor saturation dyes CY3 and CY5 (GE Healthcare Biosciences; cat. no. RPK0283 and RPK0285, respectively).

N,N-dimethylformamide, anhydrous (DMF; Sigma-Aldrich; cat. no. 227056).

! CAUTION DMF is flammable and toxic by skin contact. Wear gloves when handling. DMF should be used fresh, i.e., within 3 months after opening the bottle.

Tris-(2-carboxy-ethyl)phosphine hydrochloride (TCEP; Sigma-Aldrich; cat. no. C4706).

Immobiline DryStrip gels, 24 cm, pI 4–7 (GE Healthcare Biosciences; cat. no. 17-6002-46).

Immobiline DryStrip Cover Fluid (GE Healthcare Biosciences; cat. no. 17-1335-01).

Agarose Prep (GE Healthcare Biosciences; cat. no. 80-1130-07).

Bromophenol Blue (GE Healthcare Biosciences; cat. no. 17-1329-01).

30% (w/v) acrylamide, 0.8% (w/v) N,N′-methylenebis-acrylamide (Wako; cat. no. 016-15915).

! CAUTION Acrylamide is highly toxic. Wear gloves when handling.

Tris-HCl buffer 1.5 M, pH 8.8 (BioRad; Hercules, CA; cat. no. 161-0798).

Glycerol, 87% (GE Healthcare Biosciences; cat. no. 17-1325-01).

Ammonium persulfate (APS; GE Healthcare Biosciences; cat. no. 17-1311-01).

! CAUTION APS is harmful if inhaled or swallowed.

N,N,N,N′-tetra-methyl-ethylenediamine (TEMED; GE Healthcare Biosciences; cat. no. 17-1312-01).

! CAUTION TEMED is harmful if inhaled or swallowed.

Tris-(hydrocymethyl)aminomethane (Tris; 5 kg; Wako; cat. no. 017-16383)

Glysine (10 kg, Wako; cat. no. 073-00737).

Sodium dodecyl sulfate (SDS; Wako; cat. no. 191-07145).

! CAUTION SDS may cause irritation of the respiratory tract, eyes, and skin. Wear gloves and mask when handling.

Bind-Silane (GE Healthcare Biosciences; cat. no. 17-1330-01).

! CAUTION Bind-Silane is flammable and toxic by skin contact. Wear gloves when handling.

Acetic acid, HPLC grade (Wako; cat. no. 017-00251).

! CAUTION Acetic acid is toxic by skin contact. Wear gloves when handling.

Methanol, HPLC grade (Wako; cat. no. 138-06473).

! CAUTION Methanol is toxic by skin contact. Wear gloves when handling.

Acetonitrile, HPLC grade (Sigma-Aldrich; cat. no. 27072-7).

! CAUTION Acetonitrile is flammable and toxic by skin contact. Wear gloves when handling.

Ammonium bicarbonate (Sigma-Aldrich; cat. no. A6141).

Trifluoroacetic acid, HPLC grade (TFA; Wako; cat. no. 202-10733).

! CAUTION TFA is flammable and toxic by skin contact. Wear gloves when handling.

Sequence-grade modified trypsin (Promega; Madison, WI, USA; cat. no. V5111).

Trichloroacetic acid (TCA; Wako; cat. no. 200-08005).

! CAUTION TCA may cause irritation of the respiratory tract, eyes, and skin. Wear gloves when handling.

▲ CRITICAL All reagents used in the protocol should be of the highest quality.

EQUIPMENT

LASIK system (EC-5000 CXIII; Nidek; Gamagori, Japan).

CO_2 incubator (Thermo Scientific; Yokohama, Japan).

Porous polyethylene terephthalate (PET) membranes (BD; cat. no. 353181).

NIH3T3 murine fibroblast cells (ATTC; Manassas, VA, USA).

MDA-MB-231 human breast cancer cells (ATTC).

Excimer laser (193 nm, 10 Hz) EC-5000 CXIII (Nidek; Gamagori, Japan).

Light microscope (BX51, Olympus; Tokyo, Japan).

CCD camera DP72 (Olympus).

Immobiline Drystrip Reswelling Tray for 7–24 cm IPG strips (GE Healthcare Biosciences; cat. no. 80-6465-32).

IEF electrode strips (GE Healthcare Biosciences; cat. no. 18-1004-40).

Filter paper (chromatography paper 3MM CHR; Whatman, Brentford, Middlesex, UK; cat. no. 3030-909).

Multiphor II electrophoresis unit (GE Healthcare Biosciences; cat. no. 18-1018-06).

Circulator LTB-250 (AS ONE; Osaka, Japan).

EPS 3501 XL power supply (GE Healthcare Bio-sciences; cat. no. 18-1130-05).

Multimeter.

Cell culture dishes (100 × 20 mm; Corning Inc.; Corning, NY, USA; cat. no. 430167).

Shaker SRR-2 (AS ONE).

Equilibration tube set (GE Healthcare Biosciences; cat. no. 80-6467-79).

DALT Gradient Maker with a peristaltic pump (GE Healthcare Biosciences; cat. no. 80-6067-65).

GiantGelCaster (BIO CRAFT; Tokyo, Japan).

Low-fluorescence glass plates (BIO CRAFT).

Ettan DALT Cassette Rack (GE Healthcare Bio-sciences; cat. no. 80-6467-98).

Spacers for SE 250 and SE 260 Mini-Vertical gel units (10.5 cm × 1.80 mm × 0.75 mm; GE Healthcare Biosciences; cat. no. 80-6149-92).

GiantGelRunner with a dark box (BIO CRAFT); a large vertical electrophoresis apparatus with a cooling system plus a dark box to run gels in the dark.

Thermo Circulator ZL-100 (TAITEC; Saitama, Japan).

DarkBox for gel storage (BIO CRAFT).

Typhoon Trio (GE Healthcare Biosciences; cat. no. 63-0055-87).

KIMTECH Pure CL4 (Kimberly-Clark; Roswell, GA; cat. no. 7605).

Crew Wipes (Sigma-Aldrich; cat. no. Z23681-0).

Deep freezer (−80 °C).

DeCyder 2-D differential analysis software v 4.0, 5.0 or 6.0 (GE Healthcare Biosciences).

Data-mining software for DNA microarray data analysis: Expressionist (GeneData; Basel, Switzerland) and GeneMaths XT (Applied Maths; Sint-Martens-Latem, Belgium).

Reference markers sheet (GE Healthcare Bio-sciences; cat. no. 18-1143-34).

Large gel picker PG-100 (AS ONE).

96-well thin-wall plates (Asahi Techno Glass).

FT latex gloves, 400 mm (TGK; Tokyo, Japan).

Ultrasonic cleaner (AS ONE).

BioShaker MBR-022 (AS ONE).

AES2010 SpeedVac system (Thermo Electron Corp.; Waltham, MA, USA).

Hitech Tube Crystal (HiTech; Tokyo, Japan; cat. no. M-50001).

Cell scraper (Corning Inc.; cat. no. 3010).

TRIzol® RNA Isolation Reagents (Invitrogen; cat. no. 15596-026).

Chloroform (Wako; cat. no. 038-02606).

Isopropyl alcohol (Wako; cat. no. 164-08335).

70% ethanol (Wako; cat. no. 057-00456).

DEPC water (Invitrogen; cat. no. 750024).

SuperScript III First-Strand Synthesis System for RT-PCR (Invitrogen; cat. no. 18080-051).

KOD -Plus- Neo (TOYOBO; Osaka, Japan; cat. no. KOD-401).

TArget CloneTM -Plus- (TOYOBO; cat. no. TAK-201).

Competent high DH5α (TOYOBO; cat. no. DNA-903).

Bacto-tryptone (BD; cat. no. 211705).

Bacto-yeast extract (BD; cat. no. 212750).

NaCl (Wako; cat. no. 191-01665).

1N NaOH (Wako; cat. no. 192-02175).

Bacto-agar (Wako; cat. no. 010-08725).

Ampicillin solution (Wako; 012-20162).

IPTG (TaKaRa; Shiga, Japan; cat. no. 9030).

0.22-μm filter (Millipore; Billerica, MA, USA; cat. no. SLGP033RS).

5-bromo-4-chloro-3-indolyl-β-D-galactoside (X-gal) (TaKaRa; cat. no. 9031).

N,N-dimethyl-formamide (Wako; cat. no. 045-29192).

Restriction enzymes (New England BioLabs; Ipswich, MA, USA).

PCI (phenol:chloroform:isoamyl alcohol, 25:24:1) (Sigma-Aldrich; cat. no. P2069).

CI (chloroform:isoamyl alcohol, 24:1) (Fluka; cat. no. 25666).

QIAquick Gel extraction kit (Qiagen; Venlo, Netherlands; cat. no. 28704).

TE buffer (Wako; cat. no. 314-90021).

Lipofectamine® LTX and PLUS™ Reagents (Invitrogen; cat. no. 15338-100).

Opti-MEM® I Reduced Serum Medium (GIBCO; cat. no. 31985-062).

Bovine serum albumin (Sigma-Aldrich; cat. no. A4503).

Phalloidin (Sigma-Aldrich; cat. no. P1951).

IgG antibody (Jackson ImmunoResearch; West Grove, Pennsylvania, USA; cat. no. 567-78451).

FV1000D IX81 confocal scanning system (Olympus).

REAGENT SETUP

Complete culture medium: L-15 supplemented with 10% FBS, 100 units/mL penicillin, 100 μg/mL streptomycin, and 0.3 g/L L-glutamine.

Conditioned medium: culture NIH3T3 cells to confluence, replace the medium with FBS-free DMEM, and maintain the cells for an additional 3 days; collect and filter the culture medium and store as the conditioned medium at −80 °C.

Triton X-100 (10%): dissolve 10 mL of Triton X-100 in 70 mL of MilliQ water, make up to 100 mL with MilliQ water, and store at room temperature (~25 °C) until use.

Lysis buffer: 50 mM Tris-HCl (pH 7.4), 150 mM NaCl, 1% Triton X-100, 20 mM ethylenediamine tetraacetic acid, and protease inhibitor cocktail in MilliQ water.

Urea lysis buffer: 6 M urea, 2 M thiourea, 3% (w/v) CHAPS, 1% (v/v) Triton X-100. Dissolve 105 g urea, 38.05 g thiourea, 7.5 g CHAPS, and 25 mL Triton X-100 in 200 mL MilliQ water, make up to 250 mL with MilliQ water. Add 3 g Amberlite IRN-150K and stir for several hours; filter through Whatman paper. Aliquot and store at −80 °C until use.

Cy3 and Cy5 dye solution for analytical gels: centrifuge a tube containing 300 nmol powdered CyDye DIGE Fluor saturation dye at 694 × *g* for 5 min. Add 60 μL DMF to final concentration of 5 nmol/μL, vortex and centrifuge at 694 × *g* for 10 s. Store at −20 °C until use.

Cy3 and Cy5 solutions for preparative gels: centrifuge a tube containing 300 nmol powdered CyDye DIGE Fluor saturation dye at 694 × *g* for 5 min. Add 20 μL DMF (final concentration 15 nmol/μL), vortex and centrifuge the tube at 694 × *g* for 10 s. Store at −20 °C until use.

TCEP solution for the analytical gels: dissolve 28 mg TCEP in 50 mL MilliQ water just before use.

TCEP solution for the preparative gels: dissolve 28 mg TCEP in 5 mL MilliQ water just before use.

DTT stock solution: dissolve 1 g DTT in 4 mL MilliQ water. Store at −80 °C until use.

2× urea lysis buffer: 6 M urea, 2 M thiourea, 3% (w/v) CHAPS, 1% (v/v) Triton X-100, 130 mM DTT, 2% (v/v) Pharmalyte 3–10. Mix 900 μL urea lysis buffer, 80 μL DTT stock solution, and 20 μL Pharmalyte; make up to 1000 μL with MilliQ water.

1× urea lysis buffer: 6 M urea, 2 M thiourea, 3% (w/v) CHAPS, 1% (v/v) Triton X-100, 65 mM DTT, 1% (v/v) Pharmalyte 3–10. Mix 900 μL urea lysis buffer, 40 μL DTT stock solution and 10 μL Pharmalyte; make up to 1000 μL with MilliQ water.

Internal control sample: prepare the internal control sample by mixing equal amounts of protein extracts from pseudopodia and cell bodies.

SDS (10%): dissolve 50 g SDS in 300 mL MilliQ water, make up to 500 mL with MilliQ water. Store at room temperature.

Equilibration buffer: for 12 IPG gel (24 cm length), mix 90 g urea, 17 mL 1.5 M Tris-HCl (pH 8.8), 87 mL 87% glycerol, 25 mL 10% SDS. Make up to 250 mL with MilliQ water. Stir the solution for several hours until it reaches room temperature. Add 1.25 g DTT just before use.

Agarose sealing solution: mix 1.0 g agarose prep, 200 mL SDS-PAGE electrode buffer, 200 μL of 25 mg/mL bromophenol blue (BPB). Heat the solution in a microwave oven,